International Journal For Advanced Research In Science & Technology
A peer reviewed international journal
www.ijarst.in
ISSN: 2457-0362

Wind Energy Conversion System with Fuzzy Logic Based Solid State Transformer

Rayapalyam Kranthe[1], M.Tech, Department of EEE, Swetha Institute of Technology & Science, Tirupati,AP

Dr. E. Kiran Kumar[2], Prof, Department of EEE, Swetha Institute of Technology & Science, Tirupati,AP.

Abstract: In wind energy conversion systems, the fundamental frequency step up transformer acts as a key interface between thewind turbine and the grid. Recently, there have been efforts toreplace this transformer by an advanced power electronics basedsolid state transformer (SST). This paper proposes a configurationthat combines the doubly fed induction generator based wind turbineand Fuzzy Logic Based SST operation. The main objective of the proposed configurationis to interface the turbine with the grid while providingenhanced operation and performance. In this paper, SST controlsthe active power to/from the rotor side converter, thus, eliminatingthe grid side converter. The proposed Fuzzy Logic Controller system meets the recent gridcode requirements of wind turbine operation under fault conditions. Additionally, it has the ability to supply reactive power tothe grid when the wind generation is not up to its rated value. Adetailed simulation study is conducted to validate the performanceof the proposed configuration. MATLAB/SIMULINK Results shows the effectiveness of the proposed SST based DFIG System.

Index Terms—doubly fed induction generator, fault ride through, power electronic transformer, solid-state transformer.

I. INTRODUCTION

Over the last decade, the penetration of renewable energy sources has been increasing steadily in the power system. In particular, wind energy installations have grown rapidly with global installed capacity increasing from 47.6 GW in 2004 to369.6 GW in 2014 [1]. Amongst the many technologies that exist for wind energy conversion systems (WECS), doubly fed induction generators (DFIG) have been prevalent due to variable speed operation, high power density and lower cost [2], [3]. DFIG based WECS consist of an induction generator whose stator is directly connected to the gridwhile its rotor is connected via back to back converters known as the rotor side converter (RSC) and grid side converter (GSC), respectively [3]. The generator is normally operated at a range of 500 V–700 V and is connected to the transmission network (11–33 kV) through a transformer that acts as an integral part of the WECS to interface the wind turbine and the grid. Recently, there has been much interest in developing an alternative to the traditional fundamental frequency transformer using solid-state devices.

International Journal For Advanced Research In Science & Technology
A peer reviewed international journal
www.ijarst.in
ISSN: 2457-0362

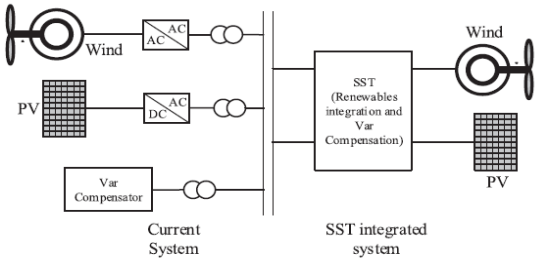

Fig. 1 Expected SST integrated grid.

The solid-state transformer (SST) achieves voltage conversion through a series of power electronics devices while offering multiple advantages, such as, smaller size, improved power quality and fault tolerant features [4]–[11]. Fig. 1 shows a power distribution system based on SST as envisioned in [4]. Proposed in 1980 [5], advances in solid-state technology have made SST more viable today leading to increased research in its feasibility and physical realization. A promising 10 kVA prototype has been developed and presented in [6]. Further, the use of high voltage silicon carbide (SiC) power devices for SST has been explored and presented in [7], [8]. As seen in Fig. 1, SST can act as an interface between the grid and generation sources. However, research showing detailed configurations for integrating existing technologies is limited. In [9], work is reported on using SST in a microgrid based on renewable sources. In [10], SST is used to interface a wind park based on squirrel cage induction generator (SCIG) with the grid. However, a detailed analysis on fault ride through requirement and reactive power support has not been conducted in [10].

In this paper, a new configuration is proposed that combinesthe operation of DFIG based WECS and SST. This configuration acts as an interface between the wind turbine and grid while eliminating the GSC of DFIG. Moreover, it is essential to have fault ride through (FRT) incorporated in DFIG system to meet the grid code requirements [11]–[20]. In the proposed work, the developed configuration allows DFIG to ride through faults seamlessly, which is the aspect (FRT) that has not been addressed in the earlier work on SST interfaced WECS.

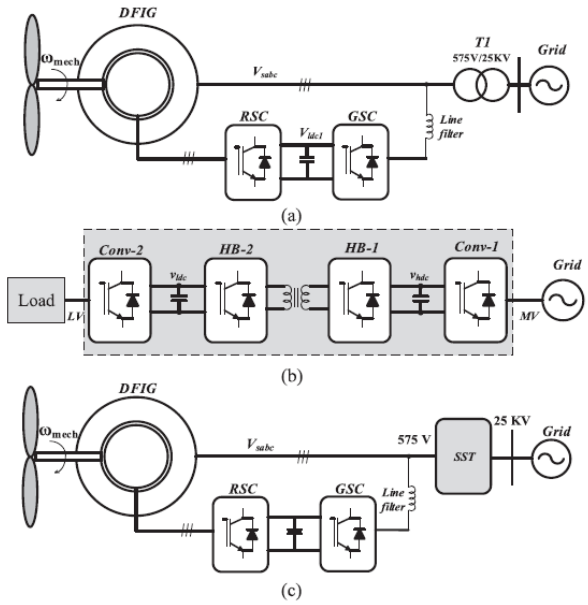

Fig. 2 (a) Regular DFIG configuration, (b) SST structure and (c) configuration suggested in [10].

II. PROPOSED SYSTEM CONFIGURATION AND MODELING

A. Motivation for DFIG

In [21], it has been reported that a DFIG based wind turbineis the lightest amongst the current wind systems which also explains its wide commercial use. Moreover, in the proposed configuration, the GSC present in traditional DFIG systems is removed making the machine setup further lighter. On the other hand, SST being used in anAC/AC system is expected to be 25% smaller in volume than traditional low frequency transformer [22]. Thus, the use of SST to interface a DFIG based wind system can be expected to provide further reduction

International Journal For Advanced Research In Science & Technology
A peer reviewed international journal www.ijarst.in
ISSN: 2457-0362

in weight and volume when compared to other wind systems with the fundamental frequency transformer.

B. Background

The widely used DFIG based WECS configuration is shownin Fig. 2(a). The stator terminals of the machine are connected directly to the grid while the rotor terminals are connected via back to back converters. The RSC allows for variable speed operation of the machine by injecting or drawing active power from the rotor. The GSC maintains the DC link by transferring the active power from the rotor to the grid or vice versa. The step up transformer T1, is the interface between the DFIG system and grid.

Three stage SST configuration is shown in Fig. 2(b), whereit connects the grid to a distribution load. Conv-1 is a fully controlled three-phase converter connected to the high voltage grid (11–33 kV). It draws real power from the grid and maintains the high voltage DC bus (*v*hdc). This high voltage DC isconverted to high frequency AC voltage by a half bridge converter(HB-1) which is then stepped down using a smaller sized high frequency transformer. This transformer provides the galvanic isolation between the grid and load. A second half bridge converter (HB−2) converts the low voltage AC to low voltage DC voltage (*v*ldc). This DC bus supports conv-2 which maintains the three-phase/single phase supply voltage to the load by producing a controlled three phase voltage. The configuration thus performs the function of a regular transformer allowing for bi-directional power flow using a series of power electronics devices [5]–[10].

As mentioned earlier, the use of SST in WECS has been exploredby Xu *et al.* in [10]. SST was used in an SCIG based WECS replacing the step-up transformer between the turbine and grid. It was shown that SST can improve the voltage profile at the terminals of the SCIG. While the focus of [10] was on SCIG, possible configuration for DFIG systems was also showcased that is represented in Fig. 2(c). The step-up transformer T1 in Fig. 2(a) is directly replaced by the SST in Fig. 2(c).

C. Proposed System Description

The general DFIG based WECS representation is shown inFig. 3(a) whereas the proposed system configuration is shown in Fig. 3(b). In the proposed configuration, the fundamental frequency transformer is replaced by the SST. The proper control of SST converter that is close to the stator of DFIG, addressed as machine interfacing converter (MIC), can aid the machine in its operation. Thus, it is proposed to eliminate the GSC in the DFIG system configuration by incorporating its role in SST. Note that this new arrangement modifies the overall operation and control of standard GSC-RSC based DFIG system. In principle, the machine terminal voltages can be maintained constant in spite of any voltage variations in the grid using MIC. The direction of power flow in the proposed configuration occurs from the low voltage machine terminals to the grid. The MIC is responsible for: (*i*) maintaining the required voltages at the stator terminals and (*ii*) transferring the real power from the stator terminals (*Ps*) to the low voltage DC bus (*v*ldc). This low voltage DC bus is regulated by the high frequency stage converters (HB1 and HB2) and not by the DFIG. In other words, MIC acts as a stiff grid at the stator terminals. Interestingly, the low voltage DC bus (magnitude) is very close to

International Journal For Advanced Research In Science & Technology
A peer reviewed international journal
www.ijarst.in
ISSN: 2457-0362

the one controlled by GSC in the regular DFIG configuration [*v*ldc1 in Fig. 2(a)]. This allows the RSC in the proposed configuration to be connected directly to *v*ldc of SST. The *v*ldc has two functions, namely, (*i*) to transfer active power from the stator terminals to the grid and (*ii*) to transfer active power (*Pr*) to/from the RSC during sub-synchronous or super-synchronous operation.

The power transfer through the high frequency stage, fromthe low voltage DC bus to the high voltage DC bus (*v*hdc), is controlled by introducing a phase shift between the two high frequency AC voltages with the objective of regulating the DCbus voltage (*v*ldc). The grid interfacing converter (GIC) connects SST to the grid and maintains the DC link (*v*hdc) by exchanging active power with the grid.

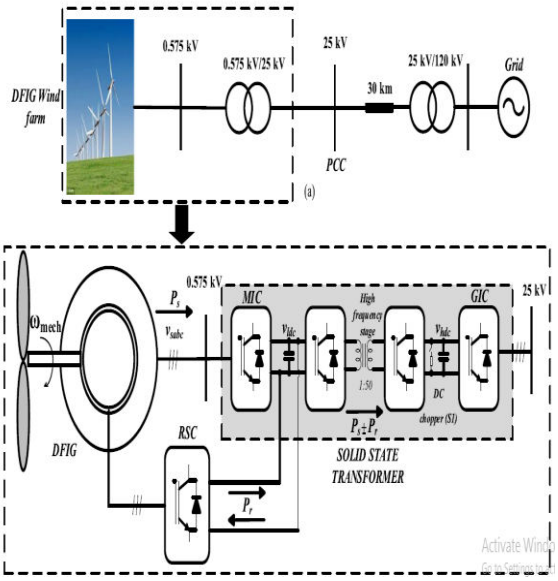

Fig. 3. (a) Regular DFIG configuration and (b) Proposed SST based DFIG configuration.

To provide an effective FRT in the proposed configuration, aDC chopper is incorporated at *v*hdc bus. During the grid fault conditions, the power being generated by the wind turbine is evacuated through the high frequency stage into theDCchopper. Further, the high frequency stage continues to maintain the low voltage DC bus (*v*ldc), allowing the voltages at the machine terminals to be constant. The presence of GIC further helps to achieve the recent grid code requirements of reactive current injection without requiring any additional control or device.Furthermore, the GIC can provide reactive power support to the grid during low wind generation periods.

III. CONTROL OF THE PROPOSED SYSTEM

To ensure smooth operation of the proposed configuration,the control objectives and algorithms for the RSC, MIC and the GIC are discussed below and shown in Fig. 4.

A. RSC Control

The rotor side control ensures the variable speed operation ofDFIG by enabling the generator to work in super synchronous or sub synchronous modes. In super synchronous mode, the total power generated is partially evacuated through the RSC. Under sub synchronous modes, the RSC injects active power into the rotor. The RSC in the proposed converter is controlled using a decoupled $d-q$ synchronous frame reference. The *q*axis of the reference frame is aligned with the machine stator voltage. On doing this, as per (3), the torque produced by the machine can be directly controlled by controlling the *q*-axis rotor current *i*qr. Moreover, the reactive power produced at thestator terminal can also be controlled by controlling the *d*-axisrotor current *i*dr. The control schematic for the same is shown in Fig. 4. A suitable MPPT curve is used to track the optimal rotor speed and is compared with the measured rotor speed. The error is processed by a PI controller to produce the

International Journal For Advanced Research In Science & Technology
A peer reviewed international journal
www.ijarst.in
ISSN: 2457-0362

reference torque ($T*e$) for the machine. Using (3), the rotor q-axis reference current ($i*$qr) is calculated.

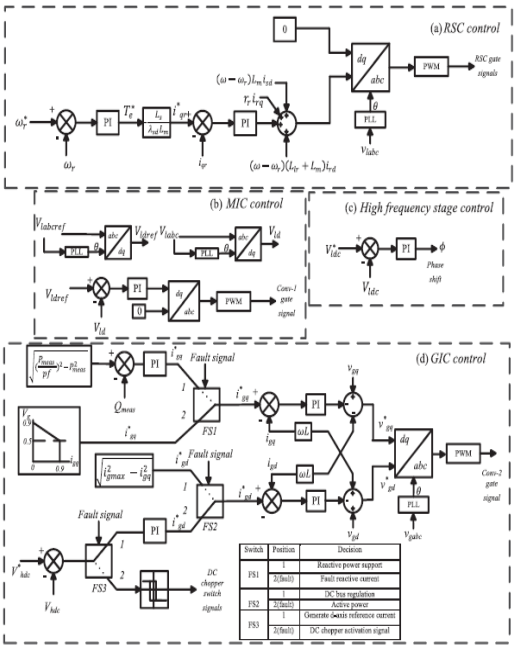

Fig. 4. Control diagram of proposed configuration.

This current is compared with the actual rotor q-axis current ($i$qr) and the error is processed by a

PI controller to generate the q-axis reference voltage ($v*$qr). Inthe proposed configuration, the stator terminals are completelydecoupled from the grid through the SST. The GIC suppliesany reactive power requirement from the grid and the machineonly generates active power. This eliminates the need for controlover the d-axis rotor current and voltage. Thus, the d-axis rotorvoltage reference for RSC ($v*$dr) is maintained as zero. The$d-q$ axis reference voltages are then converted to three phaseand used to generate the gate pulses for the RSC. Further detailsregarding the control system can be obtained in [4].

B. MIC Control

The MIC is the first stage of the SST connecting the low voltagemachine output to the high frequency stage. This converter is controlled to maintain 1 p.u. voltage (0.575 kV) at 50 Hz at the stator terminals of the machine. The control is achieved by generating a reference voltage and comparing the d-axis component of the reference ($v*$sd) with the voltage at the output of the converter ($v$sd). The power generated at the stator terminals of the machine is thus absorbed by the low voltage DC bus connected to MIC operating at 1.15 kV.

IV Fuzzy Based Feedback Controller

Fuzzy logic is a form of logic that is the extension of boolean logic, which incorporates partial values of truth. Instead of sentences being "completely true" or "completely false," they are assigned a value that represents their degree of truth. In fuzzy systems, values are indicated by a number (called a truth value) in the range from 0 to 1, where 0.0 represents absolute false and 1.0 represents absolute truth. Fuzzification is the generalization of any theory from discrete to continuous. Fuzzy logic is important to artificial intelligence because they allow computers to answer ‘to a certain degree’ as opposed to in one extreme or the other. In this sense, computers are allowed to think more 'human-like' since almost nothing in our perception is extreme, but is true only to a certain degree. Through fuzzy logic, machines can think in degrees, solve problems when there is no simple mathematical model. It solves problems for highly nonlinear processes and uses expert knowledge to make decisions.

4.1 Fuzzy Logic Controller

The fuzzy logic controller provides an algorithm, which converts the expert

International Journal For Advanced Research In Science & Technology
A peer reviewed international journal
www.ijarst.in
ISSN: 2457-0362

knowledge into an automatic control strategy. Fuzzy logic is capable of handling approximate information in a systematic way and therefore it is suited for controlling non linear systems and is used for modeling complex systems, where an inexact model exists or systems where ambiguity or vagueness is common. The fuzzy control systems are rule-based systems in which a set of fuzzy rules represent a control decision mechanism for adjusting the effects of certain system stimuli. With an effective rule base, the fuzzy control systems can replace a skilled human operator. The rule base reflects the human expert knowledge, expressed as linguistic variables, while the membership functions represent expert interpretation of those variables.

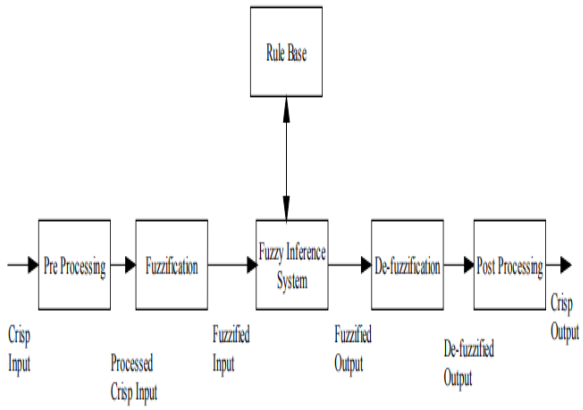

Figure 5 : Block diagram of fuzzy control system

Figure 5 shows the block diagram of fuzzy control system. The crisp inputs are supplied to the input side Fuzzification unit. The Fuzzification unit converts the crisp input in to fuzzy variable. The fuzzy variables are then passed through the fuzzy rule base. The fuzzy rule base computes the input according to the rules and gives the output. The output is then passed through de-fuzzification unit where the fuzzy output is converted to crisp output.

4.2 Hybrid Fuzzy-PID Controller

Although it is possible to design a fuzzy logic type of PID controller by a simple modification of the conventional ones, via inserting some meaningful fuzzy logic IF-THEN rules into the control system, these approaches in general complicate the overall design and do not come up with new fuzzy PID controllers that capture the essential characteristics and nature of the conventional PID controllers. Besides, they generally do not have analytic formulas to use for control specification and stability analysis. The fuzzy PD, PI, and PI+D controllers to be introduced below are natural extensions of their conventional versions, which preserve the linear structures of the PID controllers, with simple and conventional analytical formulas as the final results of the design. Thus, they can directly replace the conventional PID controllers in any operating control systems (plants, processes). The main difference is that these fuzzy PID controllers are designed by employing fuzzy logic control principles and techniques, to obtain new controllers that possess analytical formulas very similar to the conventional digital PID controllers.

4.3 Different Structures of Hybrid Fuzzy PID Controller

Han Xiong Li et.al, has proposed a two dimensional configuration for PID type FLC. In this paper optimal fuzzy reasoning model for control is proposed and is compared with conventional fuzzy control [3.14]

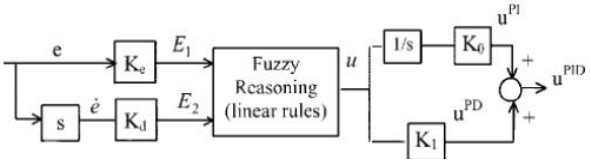

Figure 6: Architecture of fuzzy PID controller [3.14]

International Journal For Advanced Research In Science & Technology
A peer reviewed international journal www.ijarst.in
ISSN: 2457-0362

Y Zhang et.al, implemented a fuzzy PID hybrid controller for temperature control of melted aluminum in atomized furnace. In this architecture the input of fuzzy controller is error and change in error. α is the weighing factor. The total controller output is the summation of the output of fuzzy controller and PID controller. The output of Fuzzy-PID hybrid controller denoted by u is a combination of the output of fuzzy controller and the output of PID controller, symbolized as u1 and u2 respectively, involving a weighting calculation for bumpless switch between the two controllers. The weighting coefficient 'α' as a function of e can decide which controller operating mainly according to e. The fuzzy controller works mostly if e is larger than set point, or else the PID controller becomes the main controller with a bumpless switch [3.17].

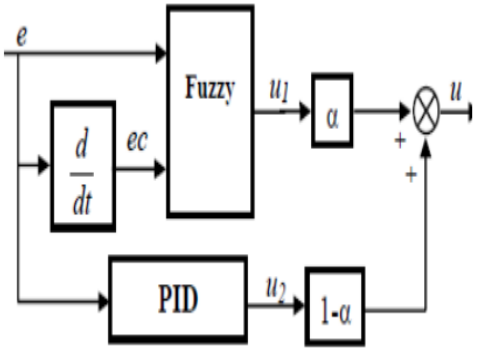

Figure 6: Architecture of fuzzy PID controller

4.4 Tuning of Fuzzy PID Controller

Seema Chopra et.al, proposed a method for tuning of fuzzy PI controller. The input scaling factors are tuned online by gain updating factor whose values are determined by fuzzy rule base [3.18]. Seema chopra et.al have proposed a neural network tuned fuzzy controller for MIMO systems from the given set of input and output data. An appropriate coupling tuned fuzzy controller is incorporated to control MIMO system to compensate for the dynamics of coupling [3.20].

6.5 Scaling Factor in Fuzzy Logic Controller

Scaling factor in a fuzzy logic controller is very important. Selection of suitable values for scaling factors are made based on the knowledge about the process to be controlled and sometimes through trial and error to achieve the best possible control performance. This is so because, unlike conventional non-fuzzy controllers to date, there is no well-defined method for good setting of scaling factors for fuzzy logic controllers. But the scaling factors are the main parameters used for tuning the fuzzy logic controller because changing the scaling factors changes the normalized universe of discourse, the domains, and the membership functions of input /output variables of fuzzy logic controller.

4.5 Hybrid Fuzzy Controller

This section gives a detail view of hybrid fuzzy controller designed to control the outlet temperature of shell and tube heat exchanger system. Figure 3.7 shows the parallel form of PID controller where all the elements (proportional, integral and derivative) are summed together to produce the control effect.

The linguistic variables used in the membership functions are described in table 3. Table 3.1: Linguistic variables in fuzzy inference system

International Journal For Advanced Research In Science & Technology
A peer reviewed international journal
www.ijarst.in
ISSN: 2457-0362

Error e(t)		Change in error Δe(t)		Controller output u(t)	
NB	Negative Big	NB	Negative Big	NB	Negative Big
NM	Negative Medium	NM	Negative Medium	NM	Negative Medium
NS	Negative Small	NS	Negative Small	NS	Negative Small
ZO	Zero	ZO	Zero	ZO	Zero
PS	Positive Small	PS	Positive Small	PS	Positive Small
PM	Positive Medium	PM	Positive Medium	PM	Positive Medium
PB	Positive Big	PB	Positive Big	PB	Positive Big

V Simulation results

To verify the effectiveness of the proposed configuration,detailed simulations are carried out. The simulated system is as represented in Fig. 7.1. A detailed model of proposed configuration is developed using the SIMULINK and SimPowerSystems toolbox in MATLAB. All the system parameters are given in Table 7.1. The performance of proposed system is evaluated under different operating conditions. All the results shown are in p.u. on a base of 5.1MVA with respective voltages.

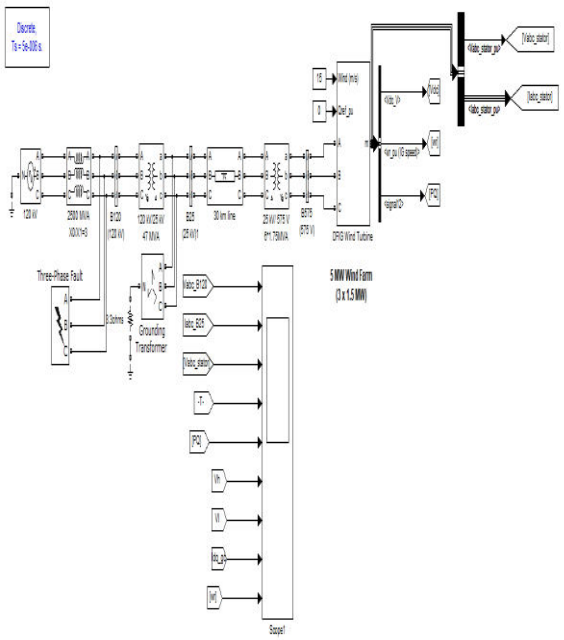

Fig 7 MATLAB/SIMULINK Model for the Prposed Fuzzy Based DFIG

A. Normal Operation

Firstly, the operation of the proposed configuration is shown under normal grid conditions in Fig. 6. In this scenario (between4.9 to 5 sec), the wind turbine is operated at a speed of 13 · m/s thus not producing peak power. The wind turbines produce a total of 4.2 MW active power. Like general DFIG, the system delivers this wind generated active power to the grid as shown in Fig. 6(e) through the SST. That is, there is no reactive power support from the GIC. Figs. 6(a) and (b) show the grid voltages and currents at the output of the GIC. Figs. 6(c) and (d) give the stator terminal voltages and machine currents at 0.575 kV.

Table 1

Parameter	Value
System Data	
Rated power	5 MVA
No. of wind turbines	3
Wind Turbine data	
Rated power	1.5 MW
Rated wind speed	15 m/s
Generator Data	
Rated apparent power	1.66 MVA
Rated voltage	0.575 kV
No of poles	6
Rated frequency	50 Hz
Stator to rotor turns ratio	575/1975
Stator resistance, Inductance	0.0023 p.u.,0.18 p.u.
Rotor resistance, inductance	0.0016 p.u.,0.16 p.u.
Inertia constant	0.685 s
SST Data	
Low voltage DC bus (v_{ldc})	1.15 kV
operating frequency	3 kHz
HF transformer turns ratio	1:50
HF transformer inductance	5.95 μH
High voltage DC bus (v_{hdc})	50 kV

The high and low voltage DC bus voltage profiles are illustratedin Figs.7(f) and (g), respectively. Fig. 7(h) provides the controlled inner loop *d*-axis and *q*-axis currents of the GIC that control the active and reactive power injection into the grid, respectively. Fig. 7(i) shows the rotor speed of the machine which remains constant at 1.2 p.u.

B. Reactive Power Support during Steady-State

The feature of using the GIC capacity to provide reactivepower support during

International Journal For Advanced Research In Science & Technology
A peer reviewed international journal
www.ijarst.in
ISSN: 2457-0362

lower wind speeds. (between time intervals of 5 sec to 5.1 sec). At 5 sec, the reactive power reference is activated to fully utilize the GIC capacity.With 13 · m⁄s wind speed (i.e. 4.2 MW), the proposed configuration can inject 2.7 MVar.

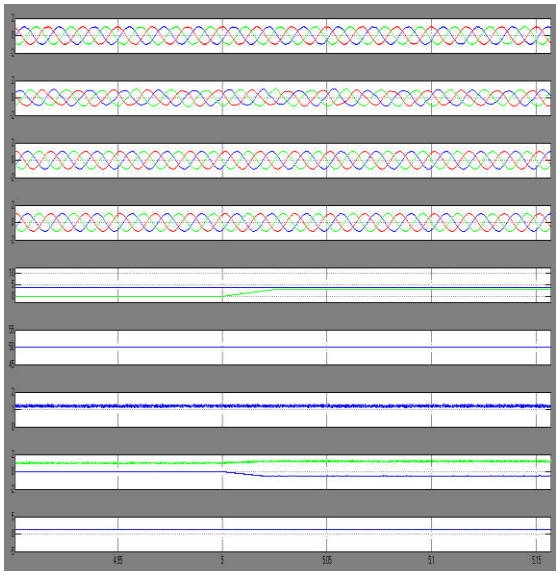

Fig 8. Normal operation of proposed configuration showing dynamics of P and Q injection. (a) Grid voltages, (b) grid currents,(c) stator terminal voltages, (d) stator currents, (e) active and reactive power injected by the system, (f) high voltage DC bus voltage, (g) low voltage DC bus voltage, (h) inner loop controlled axis grid currents and (i) rotor speed.

C. Symmetrical Fault

The performance of proposed configuration to meet FRT requirementsin recent grid codes are discussed in this section. A severe LLL-G fault is applied at upstream grid when the DFIG is producing maximum power (at 15m⁄s). The results are shown in Fig. 8. The fault is detected by sensing the positive sequence voltage magnitude. Fig. 8(a) shows the grid voltages during the fault which is introduced at 3 sec and lasts for 150 ms as per the grid code requirement. Fig. 8(b) shows the grid currents injected by the GIC. Figs.8(c) and (d) depict the stator voltage and currents of the machine, respectively. Note that the turbine does not see any change in the operating condition as MIC maintains the rated stator voltages despite the severe fault condition.

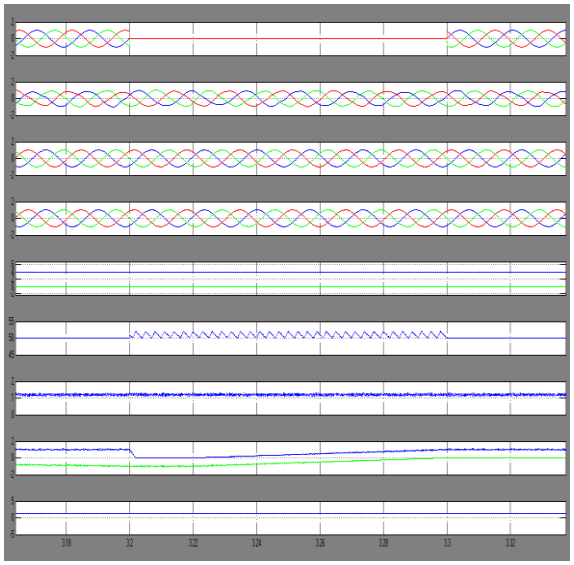

Fig. 9(f) shows the low voltage DC bus which remains Fig 7.3. Performance of the proposed configuration under three-phase symmetrical LLL-G fault. (a) Grid voltages, (b) grid currents, (c) stator terminal voltages, (d) stator currents, (e) inner loop controlled axis grid currents, (f) low voltage DC bus (g) high voltage DC bus voltage and (h) rotor speed constant.

Further, as seen from Fig. 9(g), the DC chopper evacuates the active power generated by the turbines successfully. Thus, in the proposed configuration, turbines seamlessly ride through the grid fault. On the grid side, the GIC is controlled to inject necessary reactive current to meet the grid codes. Fig. 8(e) shows the *d* and *q*-axis currents of the GIC, *i*gd and *i*gq, respectively. In pre-fault conditions it can be seen that *i*gd is at 1 p.u. since the wind turbine is operated at maximum capacity. The *q*-axis current *i*gq

International Journal For Advanced Research In Science & Technology
A peer reviewed international journal
www.ijarst.in
ISSN: 2457-0362

on the other hand is at zero as no reactive power is being injected. At 3 sec, when the fault occurs, the fault switch (FS2) is set to position 2 and the reactive current reference $i*$gq is calculated as per (6). The GIC, thus, injects 0.9 p.u. reactive current that can be seen in Fig. 9(e). The *d*-axis current ($i$gd)is calculated as per (7).

D. Unsymmetrical Fault Condition

The performance of the proposed configuration is tested under unsymmetrical faults condition as well. A single phase L-G fault is applied at the upstream grid when the DFIG is producing maximum power (15m⁄s). Fig. 10 (a) shows the grid voltages when the fault occurs at 3 sec and lasts for 150 ms. Fig. 10(b) shows the grid currents injected by the GIC. Note that the currents remain symmetrical despite the unsymmetrical fault. Figs. 10(c) and (d) show the stator voltages and currents which remain undisturbed as the MIC maintains rated stator voltages similar to the symmetrical case.

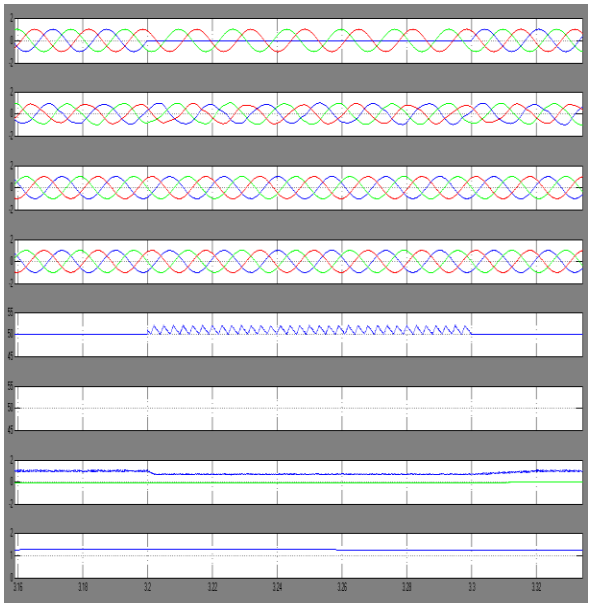

Fig 10 Performance of the proposed configuration under three-phase unsymmetrical L-G fault. (a) Grid voltages, (b) grid currents,(c) stator terminal voltages, (d) stator currents, (e) inner loop controlled axis grid currents, (f) low voltage DC bus (g) high voltage DC bus voltage and (h) rotor speed.

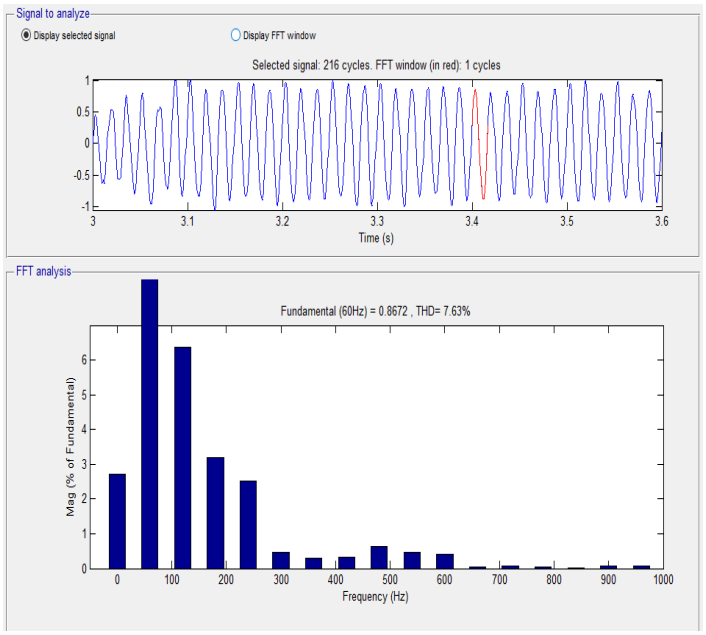

Fig 11 Total Harmonic Distrotion (THD) of the Grid Cuurnet in %

Fig. 10(a) shows the grid voltages when the fault occurs at 3 sec and lasts for 150 ms. Fig. 10(b) shows the grid currents injected by the GIC. Note that the currents remain symmetrical despite the unsymmetrical fault. Figs. 10(c) and (d) show the stator voltages and currents which remain undisturbed as the MIC maintains rated stator voltages similar to the symmetrical case.

Fig. 7.4(f) shows the low voltage DC bus. Fig. 10(g) shows the chopped DC bus voltage. Note that during a single phase fault, active power is still being transferred to the grid and the amount of power evacuated through the DC chopper is lesser than the case of a severe three phase fault. During this fault, the positive sequence voltage drops to 0.8 p.u. giving the reactive reference current ($i*$gq) as 0.4 p.u. The reactive *d* and *q* axis

International Journal For Advanced Research In Science & Technology
A peer reviewed international journal www.ijarst.in
ISSN: 2457-0362

currents, *i*gdand *i*gq are shown in Fig. 10(e), respectively.

CONCLUSION

In this thesis, a new system configuration that combines DFIG and SST operation has been proposed. This configuration replaces the regular fundamental frequency transformer with advanced power electronics based SST. The key features of the proposed configuration are outlined: Replacement of regular fundamental frequency transformer with SST leading to smaller footprint. Direct interface with SST to inject active power. Elimination of GSC in a standard DFIG system as the active power to/from RSC is regulated by MIC. Simplified DFIG control as machine supports only active power. The reactive power is supported by GIC during both normal and fault conditions. Seamless fault ride through operation during both symmetrical and unsymmetrical faults as per the latest grid codes.

REFERENCES

1. X. She, R. Burgos, G. Wang, F. Wang, A.Q. Huang, "Review of solid state transformer in the distribution system: From components to field application," in *Proceedings of the IEEEEnergy Conversion Congress and Exposition*, ECCE 2012, pp. 4077–4084, Sept., 2012.

2. J. W. Kolar, G. Ortiz, "Solid-state-transformers: Key components of future traction and smart grid systems," in *Proceedings of the International Power Electronics Conference*, IPEC 2014, Japan, May 18-24, 2014.

3. G. Ortiz, J. Biela, J. W. Kolar, "Optimized design of medium frequency transformers with high isolation requirements," in *Proceedings of the 36thIEEE Industrial Electronics SocietyConference*, IECON 2010, pp. 631-638, November 2010.

4. G. Ortiz, M. Leibl, J.W. Kolar, O. Apeldoorn, "Medium frequency transformers for solid-state-transformer applications — Design and experimental verification," in *Proceedings ofthe 10th IEEE International Conference on Power Electronics and Drive Systems*, PEDS 2013, pp. 1285–1290, April 2013

5. S. Falcones, X. Mao, R. Ayyanar, "Topology Comparison for Solid State Transformer Implementation," *IEEE Power and Energy Society General Meeting*, pp. 1-8, Jul. 2010.

6. T. Zhao, "Design and control of a cascaded h-bridge converter based solid state transformer (SST)," Ph.D. dissertation, Dept. Elect. Eng., North Carolina State Univ., Raleigh, North Carolina, USA, 2010.

7. Y. Du, S. Baek, S. Bhattacharya, A. Q. Huang, "High-voltage high-frequency transformer design for a 7.2kV to 120V/240V 20kVA solid state transformer," in *Proceedings of the 36thAnnual Conference on IEEE Industrial Electronics Society*, IECON 2010, pp. 493-498, Nov.2010.

8. B. Cougo, J. W. Kolar, "Integration of Leakage Inductance in Tape Wound Core Transformers for Dual Active Bridge Converters," in *Proceedings of the 7thInternationalConference Integrated Power Electronics Systems* (CIPS), 2012, pp. 1-6, March 2012.

9. N. Soultau, H. Stagge, R. W. De Doncker, O. Apeldoorn, "Development and demonstration of a medium-voltage high-power DC-DC converter for DC distribution systems," in *Proceedings of the 5th IEEE*

International Symposium on Power Electronics for Distributed Generation Systems, PEDG 2014, pp. 1-8, June 2014. J. Mühlethaler, J. Biela, J.W. Kolar, A. Ecklebe, "Improved core-loss calculation for magnetic components employed in power electronic systems," *IEEE Transactions on PowerElectronics*, vol. 27, no. 2, pp. 964–973, February, 2012.

[10] R. Garcia, A. Escobar-Mejia, K. George, J.C. Balda, "Loss comparison of selected core magnetic materials operating at medium and high frequencies and different excitation voltages," in *Proceedings of the Power Electronics for Distributed Generation Systems*, PEDG 2014, pp. 1-6, June 2014.

[11] G. Ortiz, J. Biela, J. W. Kolar, "Optimized design of medium frequency transformers with high isolation requirements," in *Proceeding of the 36th IEEE Industrial Electronics SocietyConference*, IECON 2010, pp. 631-638, Nov. 2010.

[12] W.G. Hurley, W. H. Wöfle, J. G. Breslin, "Optimized transformer design: Inclusive of high-frequency effects," *IEEE Transactions on Power Electronics*, vol. 13, no. 4, pp. 651-659, July 1998.

[13] R.W.A.A. De Doncker, D.M. Divan, M.H. Kheraluwala, "A three-phase soft-switched high-power-density DC/DC converter for high-power applications," *IEEE Transactions onIndustry Applications*, vol. 27, no. 1, pp. 63-73, Jan./Feb. 1991.

[14]L. G. Meegahapola, T. Littler, and D. Flynn, "Decoupled-DFIG fault ridethrough strategy for enhanced stability performance during grid faults," IEEE Trans. Sustain. Energy, vol. 1, no. 3, pp. 152–162, Oct. 2010.

[15] S. Hu, X. Lin, Y. Kang, and X. Zou, "An improved low-voltage ride through control strategy of doubly fed induction generator during grid faults," IEEE Trans. Power Electron., vol. 26, no. 12, pp. 3653–3665, Dec. 2011.

[16] P.-H. Huang, M. S. El Moursi, W. Xiao, and J. L. Kirtley, "Novel fault ride-through configuration and transient management scheme for doubly fed induction generator," IEEE Trans. Energy Convers., vol. 28, no. 1, pp. 86–94, Mar. 2013.

[17] S. Alaraifi, A. Moawwad, M. S. El Moursi, and V. Khadkikar, "Voltage booster schemes for fault ride-through enhancement of variable speed wind turbines," IEEE Trans. Sustain. Energy, vol. 4, no. 4, pp. 1071–1081, Oct. 2013.

[18] P. Kanjiya, B. B. Ambati, and V. Khadkikar, "A novel fault-tolerant DFIG-based wind energy conversion system for seamless operation during grid faults," IEEE Trans. Power Syst., vol. 29, no. 3, pp. 1296–1305, May 2014.

[19] M. Tsili and S. Papathanassiou, "A review of grid code technical requirements for wind farms," IET Renew. Power Gener., vol. 3, no. 3, pp. 308–332, Mar. 2009.

[20] E.ON Netz GmbH, "Grid code—High and extra high voltage," E.ON Netz GmbH, Bayreuth, Germany, Apr. 2006.

[21] H. Polinder, F. F. A. van der Pijl, G. J. de Vilder, and P. J. Tavner, "Comparison of direct-drive and geared generator concepts for wind turbines," IEEE Trans. Energy Convers., vol. 21, no. 3, pp. 725–733, Sep. 2006.

[22] J. E. Huber and J.W. Kolar, "Volume/weight/cost comparison of a 1 MVA 10 kV/400 V solid-state against a conventional low-frequency distribution

transformer," in Proc. IEEE Energy Convers. Congr. Expo., Sep. 2014, pp. 4545–4552.
[23] G. G. Oggier, R. Leidhold, G. O. Garcia, A. R. Oliva, J. C. Balda, and F. Barlow, "Extending the ZVS operating range of dual active bridge high-power DC-DC Converters," in Proc. 37th IEEE Power Electron. Spec. Conf., 2006, Jeju, South Korea, 2006, pp. 1–7.